Effect of Strain Nodes and Electrode Configuration on Piezoelectric Energy Harvesting From Cantilevered Beams

A. Erturk[1]
Center for Intelligent Material Systems and Structures,
Department of Engineering Science and Mechanics,
Virginia Tech,
Blacksburg, VA 24061
e-mail: erturk@vt.edu

P. A. Tarazaga

J. R. Farmer

D. J. Inman

Center for Intelligent Material Systems and Structures,
Department of Mechanical Engineering,
Virginia Tech,
Blacksburg, VA 24061

For the past five years, cantilevered beams with piezoceramic layer(s) have been frequently used as piezoelectric energy harvesters for vibration-to-electric energy conversion. Typically, the energy harvester beam is located on a vibrating host structure and the dynamic strain induced in the piezoceramic layer(s) results in an alternating voltage output across the electrodes. Vibration modes of a cantilevered piezoelectric energy harvester other than the fundamental mode have certain strain nodes where the dynamic strain distribution changes sign in the direction of beam length. It is theoretically explained and experimentally demonstrated in this paper that covering the strain nodes of vibration modes with continuous electrodes results in strong cancellations of the electrical outputs. A detailed dimensionless analysis is given for predicting the locations of the strain nodes of a cantilevered beam in the absence and presence of a tip mass. Since the cancellation issue is not peculiar to clamped-free boundary conditions, dimensionless data of modal strain nodes are tabulated for some other practical boundary condition pairs and these data can be useful in modal actuation problems as well. How to avoid the cancellation problem in energy harvesting by using segmented electrode pairs is described for single-mode and multimode vibrations of a cantilevered piezoelectric energy harvester. An electrode configuration-based side effect of using a large tip mass on the electrical response at higher vibration modes is discussed theoretically and demonstrated experimentally. [DOI: 10.1115/1.2981094]

Keywords: piezoelectricity, energy harvesting, strain nodes, electrode configuration

1 Introduction

The direct and converse piezoelectric effects of certain active materials have been employed in numerous applications of structural sensing and actuation for decades. Recently, the direct piezoelectric effect has been used for harvesting electrical energy from ambient vibrations. The goal of the research in vibration-based energy harvesting is to power small electronic components especially at remote locations to minimize or completely remove the requirement of battery replacement. Starting with the early work of Williams and Yates [1], numerous papers on vibration-to-electric energy conversion have appeared in literature [2]. Among the different transductions for vibration-to-electricity conversion (such as electromagnetic, electrostatic, and piezoelectric implementations), piezoelectric transduction has received the most attention in the past five years and comprehensive review articles are available [2–4]. Researchers from different disciplines have focused on experimental applications [2–4] as well as on modeling and optimization of the mechanics [5–9] and electronics [10,11] of piezoelectric energy harvesters. Typically, a piezoelectric energy harvester is a cantilevered beam with one or more piezoceramic (PZT)[2] layers and it is mounted on a vibrating host structure for voltage generation. The dynamic strain field induced throughout the PZT layer(s) results in an alternating voltage output across the electrodes covering the PZT layer(s), which are usually connected to a storage circuit.

Mathematically, the vibration-to-electric energy conversion mechanism of a cantilevered piezoelectric energy harvester can be investigated based on the piezoelectric constitutive laws [12] and the fundamental mechanics of materials relations [13]. The electric charge collected by the electrodes is the integral of the normal component of electric displacement over the electrode area and the electric displacement field induced in the PZT during the vibratory motion is a function of the strain distribution over its length. If the strain distribution (and therefore the respective electric displacement component) changes sign under a continuous (full) electrode pair, cancellations occur and the electric charge collected by the electrodes diminishes dramatically. Vibration modes of a cantilevered beam other than the fundamental mode (i.e., the first mode) have certain *strain nodes* where the dynamic strain distribution changes sign. Consequently, covering these strain nodes with continuous electrodes results in *cancellation* of the electrical outputs and a reduction in the energy harvested from the respective vibration modes.

In this paper, the effect of strain nodes on the electrical outputs of cantilevered harvesters is studied and how to prevent their undesired cancellation effects is addressed. First, the theory of cancellation is explained based on the electrical circuit equation of a recent distributed parameter electromechanical model [9] for cantilevered piezoelectric energy harvesters. Then, a dimensionless study is given for predicting the strain node positions of cantilevered energy harvesters. In most energy harvesting applications, a tip mass (proof mass) is used in order to tune the fundamental natural frequency of the harvester beam to a dominant excitation frequency or just to reduce its natural frequencies and increase its

[1]Corresponding author.
[2]The abbreviation PZT is used here for a generic piezoelectric ceramic, rather than a specific material.

Contributed by the Technical Committee on Vibration and Sound of ASME for publication in the JOURNAL OF VIBRATION AND ACOUSTICS. Manuscript received October 25, 2007; final manuscript received July 3, 2008; published online January 6, 2009. Assoc. Editor: William W. Clark.

Downloaded From: http://vibrationacoustics.asmedigitalcollection.asme.org/ on 09/27/2013 Terms of Use: http://asme.org/terms

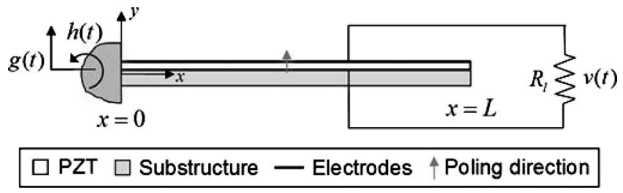

Fig. 1 Piezoelectric energy harvester under translational and small rotational base excitations

dynamic flexibility especially in microscale applications [14]. Therefore, the effect of a tip mass on the positions of the strain nodes is also investigated in a dimensionless basis. The cancellation issue caused by the presence of strain nodes is not peculiar to clamped-free boundary conditions. Since piezoelectric beams with other geometric boundary conditions (such as clamped-clamped [11] and pinned-pinned [15]) have also been investigated in the literature of energy harvesting, the strain node positions of beams with pinned-pinned, clamped-clamped, and clamped-pinned boundary conditions are tabulated for the first five vibration modes.

After the theoretical derivations and tabulations, an experimental study is provided to demonstrate the cancellation of voltage output in harvesting energy from the second vibration mode. The relationship between the discussion given here and a recent study [16,17] on piezoelectric energy harvesting from the static deflection of a clamped circular plate is also explained. How to avoid the cancellation problem in energy harvesting by using segmented electrode pairs is described for single-mode and multimode vibrations of a cantilevered piezoelectric energy harvester.

Even though simple energy harvester models assume single-harmonic excitation at the fundamental mode, in most practical cases, ambient vibration energy does not consist of a single harmonic (see, for instance, the sample frequency spectra given by Roundy et al. [5] or the random acceleration history of an automobile compressor measured by Sodano et al. [18]). Therefore, in practice, higher modes of the harvester can be excited due to the random, varying frequency, or impulse-type excitations generated by ambient vibration sources. The attachment of a tip mass makes the first mode of the cantilever more flexible by increasing its tip deflection; however, it makes the tip relatively stationary at higher vibration modes. If the tip mass is large (as in typical microscale cantilevers) so that its rotary inertia restricts the tip rotation, the free boundary acts as a clamped boundary at higher vibration modes. It is shown that using full electrodes for clamped-clamped boundary conditions is detrimental to the voltage output at higher vibration modes. An experimental demonstration is presented for the side effect of using a large tip mass on the electrical response of cantilevered piezoelectric energy harvesters at higher vibration modes.

2 Theoretical Background

2.1 Mathematical Formulation. A unimorph cantilevered piezoelectric energy harvester that is excited by the motion of its base (in the form of translation in the transverse direction $g(t)$ with superimposed small rotation $h(t)$) is shown in Fig. 1. Electromechanical modeling of cantilevered piezoelectric energy harvesters has been studied by several authors in the past five years [5–9]. Single-degree-of-freedom (SDOF) models [5,7] as well as approximate distributed parameter models [6,7] are available in literature. The origin of our discussion here is the experimentally validated [19] distributed parameter model [9] (based on the Euler–Bernoulli beam assumptions), not only because of the issues associated with SDOF modeling [8] but also because the accurate mode shape information and the information of higher vibration modes (which form the basis of the following discussion) are completely lost in such oversimplified models. For a clear discussion of the effect of strain nodes and electrode locations on the electrical outputs, we focus only on the circuit equation rather than on the resulting complete electromechanical equations. For the closed-form voltage response and coupled structural response expressions of the unimorph harvester shown in Fig. 1, the reader is referred to Ref. [9]. The implementation of the distributed parameter unimorph energy harvester model proposed by Erturk and Inman [9] to bimorph configurations as well as experimental validations can be found in Ref. [19].

As can be seen from Fig. 1, the conductive electrodes covering the top and the bottom surfaces of the PZT layer are directly connected to a resistive load (R_l) for a simple analysis. Although it is not shown as an external element, the internal capacitance of the PZT is also considered, and therefore, the circuit considered here is an *RC* circuit. However, it is not difficult to include additional linear elements (inductors, resistors, and capacitors) to the circuit in the analytical model [9]. For instance, the piezoelectric leakage resistance can be represented as a resistor parallel to the external resistive load in Fig. 1 [7]. In many cases, it is required to use a full-wave rectifier for alternating current-to-direct current (ac-dc) conversion [10,11], which results in nonlinearity in the circuit dynamics. Nevertheless, the following discussion is based on the forcing term in the electrical equation coming from the mechanical domain (as a function of vibration mode shapes). Therefore, the results of the following analysis are applicable to cantilevered harvesters, which are connected to more sophisticated circuits with the reasonable assumption that the mechanical vibration mode shapes are not affected by the circuit dynamics.

Consider the following piezoelectric constitutive relation reduced from the tensorial representation [12] for the configuration shown in Fig. 1:

$$D_3 = e_{31}S_1 + \varepsilon_{33}^S E_3 \tag{1}$$

where D_3 is the electric displacement component, e_{31} is the piezoelectric constant, S_1 is the strain component, ε_{33}^S is the permittivity component at constant strain, and E_3 is the electric field component. The piezoelectric constant e_{31} is related to more commonly used piezoelectric constant d_{31} through $e_{31}=c_{11}^E d_{31}$ where c_{11}^E is the elastic stiffness constant (i.e., Young's modulus) of the PZT layer at constant electric field. Furthermore, 1 and 3 directions in the subscripts are coincident with directions x and y in Fig. 1 and the PZT layer is poled in the thickness direction.

The average bending strain in the PZT layer can be expressed at position x and time t as

$$S_1(x,t) = -h_{pc}\frac{\partial^2 w_{\text{rel}}(x,t)}{\partial x^2} \tag{2}$$

where h_{pc} is the distance from the neutral axis of the cross section to the center of the PZT layer and $w_{\text{rel}}(x,t)$ is the transverse displacement of the beam relative to its base.

Since the individual electrodes are assumed to be perfectly conductive, a single electric potential difference can be defined across them. After expressing the electric field component $E_3(t)$ in terms of the voltage $v(t)$ across the electrodes of the PZT, i.e., $E_3(t)=-v(t)/h_p$ (where h_p is the thickness of the PZT layer), the circuit equation can be obtained from [12]

$$\frac{d}{dt}\left(\int_A \underset{\sim}{D}\cdot\underset{\sim}{n}dA\right) = -b\int_0^L\left(e_{31}h_{pc}\frac{\partial^2 w_{\text{rel}}(x,t)}{\partial x^2\partial t} + \frac{\varepsilon_{33}^S}{h_p}\frac{dv(t)}{dt}\right)dx = \frac{v(t)}{R_l} \tag{3}$$

where $\underset{\sim}{D}$ is the vector of electric displacements, $\underset{\sim}{n}$ is the unit outward normal, and b is the width of the electrode pair. Note that, in Eq. (3), it is assumed that each of the electrodes covers the entire area of the respective surface (top or bottom) of the PZT. Note that, if the electrical circuit includes more linear elements than a single resistive load, the term $1/R_l$ on the right-hand side of Eq. (3) can be replaced by the admittance of the circuit seen

Downloaded From: http://vibrationacoustics.asmedigitalcollection.asme.org/ on 09/27/2013 Terms of Use: http://asme.org/terms

across the electrodes.

One can extract the circuit equation from Eq. (3) as

$$\frac{dv(t)}{dt} + \frac{v(t)}{\tau_c} = -\frac{e_{31}h_{pc}h_p}{\varepsilon_{33}^S L}\int_0^L \frac{\partial^3 w_{\text{rel}}(x,t)}{\partial x^2 \partial t}dx \tag{4}$$

where τ_c is the time constant of the circuit as it is the multiplication of the load resistance R_l and the capacitance of the PZT, $C_p = \varepsilon_{33}^S bL/h_p$, i.e., $\tau_c = R_l C_p$. Equation (4) is a first order ordinary differential equation for voltage response across the resistive load and the integrand in the forcing term is a function of the velocity response of the beam. The elastic displacement response of the beam can be represented by an absolutely and uniformly convergent series of the eigenfunctions as

$$w_{\text{rel}}(x,t) = \sum_{r=1}^{\infty} \phi_r(x)\,\eta_r(t) \tag{5}$$

where $\phi_r(x)$ and $\eta_r(t)$ are the mass normalized eigenfunction and the modal coordinate of the clamped-free beam for the rth vibration mode, respectively. If the harvester beam is assumed to be proportionally damped [8,9], $\phi_r(x)$ is the rth eigenfunction of the undamped free vibration problem given (in the absence of a tip mass) by[3]

$$\phi_r(x) = \sqrt{\frac{1}{mL}}\left[\cosh\frac{\lambda_r}{L}x - \cos\frac{\lambda_r}{L}x - \sigma_r\left(\sinh\frac{\lambda_r}{L}x - \sin\frac{\lambda_r}{L}x\right)\right] \tag{6}$$

where m is the mass per unit length of the beam and λ_rs are the dimensionless frequency numbers (or the eigenvalues) obtained from the following characteristic equation:

$$1 + \cos\lambda\cosh\lambda = 0 \tag{7}$$

and σ_r is expressed as

$$\sigma_r = \frac{\sinh\lambda_r - \sin\lambda_r}{\cosh\lambda_r + \cos\lambda_r} \tag{8}$$

Substituting Eq. (5) into the right-hand side of Eq. (4) reduces the circuit equation to

$$\frac{dv(t)}{dt} + \frac{v(t)}{\tau_c} = \sum_{r=1}^{\infty} \varphi_r \frac{d\eta_r(t)}{dt} \tag{9}$$

where the modal coupling term φ_r is

$$\varphi_r = -\frac{e_{31}h_{pc}h_p}{\varepsilon_{33}^S L}\int_0^L \frac{d^2\phi_r(x)}{dx^2}dx = -\frac{e_{31}h_{pc}h_p}{\varepsilon_{33}^S L}\left.\frac{d\phi_r(x)}{dx}\right|_L \tag{10}$$

As can be seen from Eq. (9), the forcing function on the right-hand side is a modal summation where the contribution from the rth vibration mode is the product of φ_r and $d\eta_r(t)/dt$. The modal velocity response, $d\eta_r(t)/dt$, is also an output of the system to the base motion input and it is indeed affected by the voltage response due to backward electromechanical coupling [9,19]. A more critical term is the modal coupling term φ_r, which is not only a function of geometric, material, piezoelectric, and dielectric parameters but also the *bending slope eigenfunction* evaluated at the boundaries of the electrodes. Since each of the electrodes is assumed to be covering the entire respective surface of the PZT (top or bottom) in the above derivation, and since the slope at the clamped end of the beam is already zero, the contribution to the forcing function from the rth vibration mode simply depends on the slope at the free end, as in Eq. (10). If the electrodes cover only a certain region $x_1 \leqslant x \leqslant x_2$ over the PZT, the boundaries of the integral in Eq. (10) change and the resulting expression for φ_r becomes[4]

$$\varphi_r = -\frac{e_{31}h_{pc}h_p}{\varepsilon_{33}^S L}\left.\frac{d\phi_r(x)}{dx}\right|_{x_1}^{x_2} \tag{11}$$

According to Eq. (11), the modal electromechanical coupling term (which is a measure of the modal forcing function in the circuit equation) depends on the region covered by the electrodes on the PZT surface. Therefore, contribution to the forcing function in Eq. (9) from the rth vibration mode will be large if the difference of the slopes at the boundaries of the electrodes for that mode is large and vice versa. Depending on the locations of the electrodes, modal electromechanical coupling and therefore contribution from certain vibration modes can be large or small. If it is aimed to harvest energy from the rth vibration mode by exciting the system harmonically at the rth natural frequency (ω_r), the main contribution to the forcing function in the circuit equation will be from the rth term on the right-hand side of Eq. (9), yielding

$$\frac{dv(t)}{dt} + \frac{v(t)}{\tau_c} \cong \varphi_r \frac{d\eta_r(t)}{dt} = \varphi_r A_r e^{j\omega_r t} \tag{12}$$

where $A_r e^{j\omega_r t}$ is the modal velocity response (A_r is a complex modal constant and j is the unit imaginary number). The steady state voltage response to *modal excitation* is then

$$v(t) \cong \frac{\varphi_r A_r \tau_c}{1 + j\omega_r \tau_c} e^{j\omega_r t} \tag{13}$$

where φ_r is of practical interest since $v(t) \to 0$ as $\varphi_r \to 0$ for excitation of the harvester beam at the rth natural frequency.

It turns out from the foregoing derivation that the bending slope difference at the electrode boundaries constitutes a strong parameter in the piezoelectric energy harvesting problem. If the slopes at the boundaries of the electrodes are very close to each other for a particular mode shape, the contribution to the electrical output from that mode will be very low. Furthermore, the above derivation also shows that certain boundary conditions are not useful for harvesting energy with full electrodes (e.g., clamped-clamped). The physics behind this discussion is related to the strain distribution throughout the length of the beam. If the strain distribution over the length of the beam at a certain level from the neutral axis changes sign for a certain vibration mode, collecting the charge developed by using continuous electrodes results in cancellation of the electrical outputs in harvesting energy from that vibration mode. The mathematics of cancellation is more obvious in Eq. (10), where the integrand is the *curvature eigenfunction* (which is a measure of *bending strain*). Hence, if the curvature changes sign for a vibration mode, the net electric charge output is reduced due to cancellation of the positive and negative areas under the curvature eigenfunction in integration of the electric displacement over the electrode area. The phenomenon was discussed by Cady [20] more than 60 years ago in his study on vibrations of crystals. Later, as a *converse* piezoelectric effect application, Crawley and de Luis [21] pointed out the importance of piezoelectric actuator locations for the modal actuation force of a cantilevered beam. For improving the actuation force, they [21] suggested placing the actuators away from the positions where the phase of dynamic strain changes and they underlined the necessity of using segmented actuators for the control of flexible structures.

The positions on the beam where the bending strain distribution (at a constant level from the neutral axis) changes sign for a vibration mode are called the *strain nodes*. Since the bending strain at a point is proportional to the curvature in Euler–Bernoulli beam theory, strain nodes of a vibration mode are simply the *inflection*

[3]The effect of a tip mass is discussed in Sec. 2.3.

[4]It is assumed in the entire analysis that the width of the electrodes is identical to that of the PZT.

Downloaded From: http://vibrationacoustics.asmedigitalcollection.asme.org/ on 09/27/2013 Terms of Use: http://asme.org/terms

Table 1 Frequency numbers and dimensionless positions of the strain nodes of a cantilevered Euler–Bernoulli beam without a tip mass for the first five vibration modes

Mode	Frequency no. (λ_r)	Strain node positions on x-axis ($\bar{x}=x/L$)			
1	1.87510407	—	—	—	—
2	4.69409113	0.2165	—	—	—
3	7.85475744	0.1323	0.4965	—	—
4	10.9955407	0.0944	0.3559	0.6417	—
5	14.1371684	0.0735	0.2768	0.5001	0.7212

points of the respective eigenfunction. For a cantilevered beam, all vibration modes other than the first mode have certain strain nodes. Hence the only vibration mode of a cantilevered piezoelectric energy harvester where it is safe to use continuous electrode pairs is the first mode. A simple way of avoiding cancellation of the electrical outputs at higher vibration modes implies collecting the electric charge developed at the opposite sides of a strain node with separate electrode pairs. The leads of the segmented electrodes can be combined in the circuit in an appropriate manner as described later in this work.

2.2 Strain Nodes of a Cantilevered Beam Without a Tip Mass. The curvature eigenfunction is a direct measure of bending strain distribution and it is simply the second derivative of the displacement eigenfunction given by Eq. (6). Since the system is positive definite ($\lambda_r>0$), the positions of the strain nodes are the roots of the following equation in the interval $0<\bar{x}<1$:

$$\cosh \lambda_r \bar{x} + \cos \lambda_r \bar{x} - \sigma_r(\sinh \lambda_r \bar{x} + \sin \lambda_r \bar{x}) = 0 \tag{14}$$

where $\bar{x}=x/L$ is the dimensionless position along the beam axis. Using Eq. (14) along with Eqs. (7) and (8) gives the dimensionless positions of the strain nodes over the length of the beam for the first five modes as shown in Table 1. For convenience, the frequency numbers of the first five vibration modes are also provided in Table 1 and they can be used in the following to predict the undamped natural frequencies of the harvester beam in short circuit conditions (i.e., $R_l \to 0$):

$$\omega_r = \lambda_r^2 \sqrt{\frac{YI}{mL^4}} \tag{15}$$

where YI is the bending stiffness of the beam [9]. As can be seen from Table 1, the rth vibration mode has $r-1$ strain nodes and the only vibration mode of a cantilevered beam without strain nodes is the fundamental mode.

The normalized displacement mode shapes and the strain mode shapes of the first three vibration modes of a cantilevered beam without a tip mass are displayed in Fig. 2 along with the positions of the strain nodes for modes 2 and 3. These positions give an idea on how to locate the segmented electrodes for harvesting energy from these modes without cancellation. For instance, to avoid cancellation in harvesting energy from the second vibration mode, two electrode pairs should be used to cover the regions $0 \leqslant \bar{x} < 0.2165$ and $0.2165 < \bar{x} \leqslant 1$ separately. The voltage outputs of these electrode pairs will be out of phase with each other by 180 deg and they can be combined accordingly in the electrical circuit.

The discussion so far has focused on a cantilevered beam without a tip mass. In most applications, it is required to use a tip mass to tune the fundamental natural frequency of the harvester beam to a dominant excitation frequency or just to reduce its natural frequencies and increase its dynamic flexibility especially in microscale applications. The effect of using a tip mass on the strain nodes is investigated in the following section.

2.3 Effect of Using a Tip Mass on the Strain Nodes. If a tip mass M_t is attached rigidly at $x=L$ to the cantilevered beam shown in Fig. 1, the eigenfunctions and eigenvalues described by

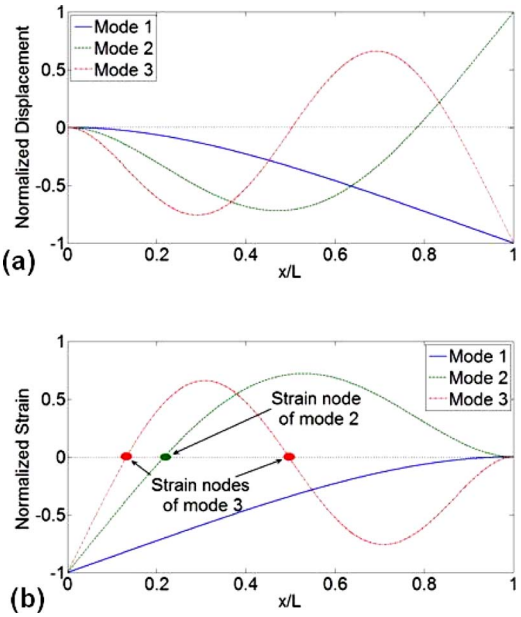

Fig. 2 (*a*) Normalized displacement and (*b*) normalized strain mode shapes of a cantilevered beam without a tip mass for the first three vibration modes

Eqs. (6) and (7) are no longer valid. If the respective differential eigenvalue problem is solved for a cantilevered beam with a tip mass, the eigenfunctions can be obtained as

$$\phi_r(x) = C_r\left[\cos\frac{\lambda_r}{L}x - \cosh\frac{\lambda_r}{L}x + \beta_r\left(\sin\frac{\lambda_r}{L}x - \sinh\frac{\lambda_r}{L}x\right)\right] \tag{16}$$

where C_r is a modal amplitude constant, which should be obtained from the orthogonality conditions for the case with a tip mass [19] and β_r is obtained from

$$\beta_r = \frac{\sin\lambda_r - \sinh\lambda_r + \lambda_r\dfrac{M_t}{mL}(\cos\lambda_r - \cosh\lambda_r)}{\cos\lambda_r + \cosh\lambda_r - \lambda_r\dfrac{M_t}{mL}(\sin\lambda_r - \sinh\lambda_r)} \tag{17}$$

The characteristic equation of the eigenvalue problem is

$$1 + \cos\lambda\cosh\lambda + \lambda\frac{M_t}{mL}(\cos\lambda\sinh\lambda - \sin\lambda\cosh\lambda) = 0 \tag{18}$$

where M_t/mL is a dimensionless parameter as it is the tip mass-to-beam mass ratio. In the above equations, the rotary inertia of the tip mass is neglected for convenience, i.e., the tip mass is considered as a point mass.

It should be noted that the curvature eigenfunction is the second derivative of Eq. (16) with respect to x. It is then possible to study the effect of a tip mass on the strain nodes in a dimensionless basis. As an example, Fig. 3(*a*) shows the variation of the displacement mode shape whereas Fig. 3(*b*) displays the variation of the strain distribution of the second vibration mode with increasing M_t/mL. The shift of the strain node position due to increasing M_t/mL is shown in Fig. 3(*b*). As the M_t/mL ratio goes from 0 to 10, the strain node of the second mode moves from $\bar{x}=0.2165$ to $\bar{x}=0.2632$.

Figure 4(*a*) shows the strain node positions of the second and the third modes versus the M_t/mL ratio. As the M_t/mL ratio increases from 0 to 10, the only strain node of the second mode moves from $\bar{x}=0.2165$ to $\bar{x}=0.2632$ whereas the two strain nodes

Downloaded From: http://vibrationacoustics.asmedigitalcollection.asme.org/ on 09/27/2013 Terms of Use: http://asme.org/terms

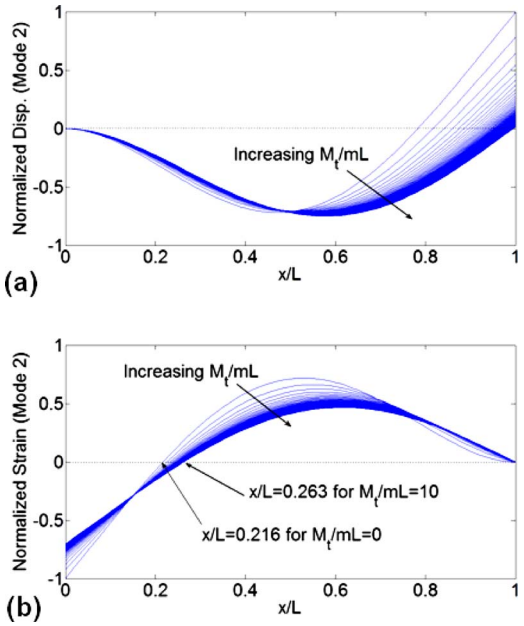

Fig. 3 Variation of the (*a*) normalized displacement and (*b*) normalized strain mode shapes of the second vibration mode with tip mass-to-beam mass ratio

of the third vibration mode move from $\bar{x}=0.1323$ and $\bar{x}=0.4965$ to $\bar{x}=0.1468$ and $\bar{x}=0.5530$, respectively. It is also useful to investigate the variation of the frequency numbers with the M_t/mL ratio, which is given in Fig. 4(*b*) for the first five vibration modes. Note that these frequency numbers give the natural frequencies when they are used in Eq. (15). As can be seen from Figs. 4(*a*) and 4(*b*), strain nodes move toward the free end of the beam and the frequency numbers decrease with increasing M_t/mL ratio. The positions of the strain nodes are more sensitive to the variations in the M_t/mL ratio in the relatively low M_t/mL region (i.e., for $0 \leq M_t/mL \leq 1$). As far as the frequency numbers are concerned, other than the frequency number of the first vibration mode, all

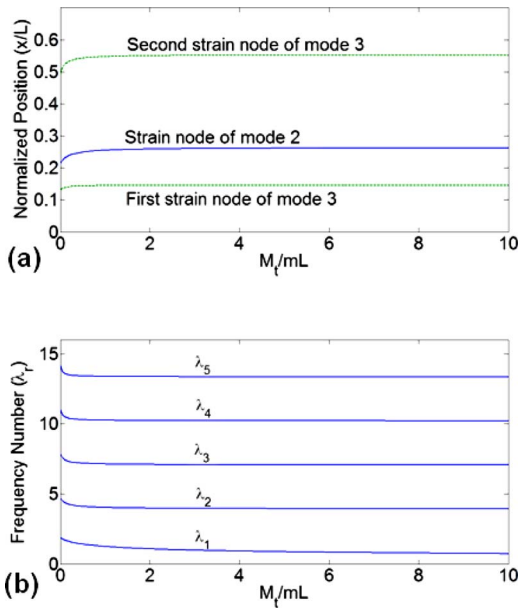

Fig. 4 (*a*) Variation of the strain node positions of the second and the third vibration modes and (*b*) variation of the first five frequency numbers with tip mass-to-beam mass ratio

frequency numbers converge to a nonzero value as $M_t/mL \to \infty$. As $M_t/mL \to \infty$, the frequency number of the rth mode of a clamped-free beam with a tip mass converges to that of the $(r-1)$th mode of a clamped-pinned beam without a tip mass[5] (except for the first frequency number λ_1, which goes to zero with a very slow rate). That the boundary conditions of a cantilevered beam with a tip mass shift from clamped-free to clamped-pinned as $M_t/mL \to \infty$ makes sense, as the rotary inertia of the tip mass is neglected. Therefore, the direct consideration of the strain nodes of a clamped-pinned beam should give a good estimate of the strain nodes for very high values of M_t/mL in modes other than the first mode. However, if the rotary inertia of the tip mass is not negligible and if it increases as $M_t/mL \to \infty$, the boundary conditions shift from clamped-free to clamped-clamped and it becomes more reasonable to estimate the strain node positions from the eigenfunctions of a clamped-clamped beam for high values of M_t/mL. Hence, it is also insightful to examine the characteristic equation of a cantilevered Euler–Bernoulli beam where the rotary inertia (I_t) of the tip mass is also considered

$$1 + \cos\lambda \cosh\lambda + \lambda\frac{M_t}{mL}(\cos\lambda \sinh\lambda - \sin\lambda \cosh\lambda) - \frac{\lambda^3 I_t}{mL^3}(\cosh\lambda \sin\lambda + \sinh\lambda \cos\lambda) + \frac{\lambda^4 M_t I_t}{m^2 L^4}(1 - \cos\lambda \cosh\lambda) = 0 \quad (19)$$

Here, the rotary inertia of the tip mass can be normalized with respect to the rotary inertia of the free rigid beam about a certain point and a similar dimensionless analysis can be performed. Equation (19) shows that the rotary inertia of the tip mass introduces two additional terms to Eq. (18). The form of the eigenfunction expression given by Eq. (16) is still the same; however, the eigenvalues to be used in Eq. (16) must be extracted from Eq. (19). As mentioned before, for a large tip mass and tip rotary inertia, the free end of the beam also acts as a clamped end. This fact is also evident from the dominating term in Eq. (19) for $(M_t/mL)(I_t/mL^3) \to \infty$, which is the characteristic equation of a uniform Euler–Bernoulli beam with clamped-clamped boundary conditions ($1-\cos\lambda \cosh\lambda=0$). According to Eq. (11), clamped-clamped boundary conditions may cause strong cancellations in the electrical outputs if full electrodes are used for covering the PZT layer(s). Therefore, employing a large tip mass for reducing the natural frequencies of a cantilevered piezoelectric energy harvester has the side effect of reducing the electrical response of the vibration modes other than the fundamental mode. This side effect of using a tip mass on the electrical response of higher vibration modes is demonstrated experimentally in Sec. 6.

2.4 Strain Nodes for Other Boundary Conditions. Since the literature of energy harvesting [11,15] and the literature dealing with piezoelectric beams [22] have considered boundary conditions other than clamped-free, the numerical data of the strain node positions for some other practical boundary conditions are tabulated in this section. Table 2 displays the positions of the strain nodes for the first five vibration modes of uniform Euler–Bernoulli beams with pinned-pinned, clamped-clamped, and clamped-pinned boundary conditions. The frequency numbers are also provided and they can be used in Eq. (15) to predict the undamped natural frequencies at short circuit conditions in each case.

Since the pinned-pinned (Table 2*a*) and clamped-clamped (Table 2*b*) boundary conditions are symmetric boundary conditions (yielding symmetric and antisymmetric mode shapes for odd

[5]The dominating term in Eq. (18) for $M_t/mL \to \infty$ is the characteristic equation of a clamped-pinned beam: $\tanh\lambda - \tan\lambda = 0$ (because the system is positive definite, $\lambda \neq 0$ in the dominating term).

Downloaded From: http://vibrationacoustics.asmedigitalcollection.asme.org/ on 09/27/2013 Terms of Use: http://asme.org/terms

Table 2 Frequency numbers and dimensionless positions of the strain nodes for Euler–Bernoulli beams with (*a*) pinned-pinned, (*b*) clamped-clamped, and (*c*) clamped-pinned boundary conditions

Mode	Freq. No. (λ_r)	Strain node positions on x-axis ($\bar{x}=x/L$)					
		(*a*) Pinned-pinned boundary conditions					
1	π	—	—	—	—	—	—
2	2π	1/2	—	—	—	—	—
3	3π	1/3	2/3	—	—	—	—
4	4π	1/4	1/2	3/4	—	—	—
5	5π	1/5	2/5	3/5	4/5	—	—
		(*b*) Clamped-clamped boundary conditions					
1	4.73004074	0.2242	0.7758	—	—	—	—
2	7.85320462	0.1321	0.5000	0.8679	—	—	—
3	10.9956079	0.0944	0.3558	0.6442	0.9056	—	—
4	14.1371655	0.0735	0.2768	0.5000	0.7232	0.9265	—
5	17.2787597	0.0601	0.2265	0.4091	0.5909	0.7735	0.9399
		(*c*) Clamped-pinned boundary conditions					
1	3.92660231	0.2642	—	—	—	—	—
2	7.06858275	0.1469	0.5536	—	—	—	—
3	10.2101761	0.1017	0.3832	0.6924	—	—	—
4	13.3517688	0.0778	0.2931	0.5295	0.7647	—	—
5	16.4933614	0.0630	0.2372	0.4286	0.6190	0.8095	—

and even modes, respectively), the positions of the strain nodes (inflection points of the mode shapes) are symmetric with respect to the center ($\bar{x}=0.5$) of the beam. However, for the clamped-pinned boundary conditions (Table 2*c*), no such symmetry exists (where $\bar{x}=0$ is the clamped boundary). It should be noted that it is safe to cover the entire surface with continuous electrodes for harvesting energy at the first vibration mode of a pinned-pinned beam since the rule for the pinned-pinned case is the same as the clamped-free case, i.e., the rth vibration mode has $r-1$ strain nodes (Table 2*a*). However, a beam with clamped-clamped boundary conditions has two strain nodes in the first vibration mode. According to Table 2*b*, the rth vibration mode of a clamped-clamped beam has $r+1$ strain nodes. Hence, three electrode pairs (with discontinuities at $\bar{x}=0.2242$ and at $\bar{x}=0.7758$) can be used to extract the electrical outputs of a clamped-clamped harvester without cancellation for vibrations with the first mode shape. Table 2*c* shows that the rth vibration mode has r strain nodes for a clamped-pinned beam. Thus, two electrode pairs (with a discontinuity at $\bar{x}=0.2642$) can handle the cancellation issue for the fundamental mode excitation of a harvester beam with clamped-pinned boundary conditions.

Among the boundary conditions investigated here, the clamped-clamped boundary condition pair constitutes a unique case. Theoretically, for excitations at all vibration modes of a clamped-clamped beam, the modal forcing term φ_r in the electrical equation and therefore the voltage response are zero, if continuous electrodes cover the entire beam surface (see Eqs. (11) and (13)). A similar issue (of total cancellation) is expected for the even vibration modes ($r=2,4,6,\ldots,2n$ where n is an integer) of the pinned-pinned case, if full electrodes cover the entire beam length. For the even modes of a beam with pinned-pinned boundary conditions, the slopes at the pinned boundaries are not zero, but they are equal to each other, theoretically, yielding a total cancellation at these modes due to Eq. (11).

The data provided in Tables 1 and 2 are also useful for modal actuation of beams with these boundary conditions because a coupling term that is similar to φ_r (given by Eq. (11)) appears in the modal equation for the beam response [9]. According to Table 1, the fundamental mode of a clamped-free beam can be excited by locating the piezoelectric actuator(s) anywhere along the beam. One should prefer a location close to the clamped end (Fig. 2(*b*)) in order to minimize the required actuation input as previously discussed by Crawley and de Luis [21]. However, excitation of the fundamental mode of a clamped-clamped beam is more critical as the piezoelectric actuator(s) should not cover the positions $\bar{x}=0.2242$ and $\bar{x}=0.7758$ (Table 2*b*). Covering one of these strain nodes with an actuator may require dramatically high voltage inputs for exciting the respective mode.

3 Experimental Demonstration

The cantilevered steel beam (with dimensions of $600\times19.1\times3.05$ mm^3) shown in Fig. 5 is used in order to demonstrate the effect of strain nodes on the voltage output. An electromagnetic shaker with a stinger is used to excite the cantilevered beam at its first two natural frequencies. Since the main purpose is to demonstrate the importance of the strain nodes on energy harvesting by using cantilevered beams with PZT layers/patches, the dimensions of the beam are selected arbitrarily and the importance is given only to justify the Euler–Bernoulli beam assumptions. Hence, the results of the following study are valid for all microscale and macroscale cantilevered piezoelectric energy harvesters, which can be modeled as thin beams.

Here, the first two vibration modes are considered for a simple demonstration of the voltage cancellation at higher vibration modes. Note that the cantilevered harvester model [9] that forms the theoretical background of this paper was experimentally validated in a recent paper [19]. Hence, the experimental demonstration of cancellation given here does not aim to verify the electrical equations given in Sec. 2.1 quantitatively. The goal of this section is to provide a qualitative verification of voltage cancellation for

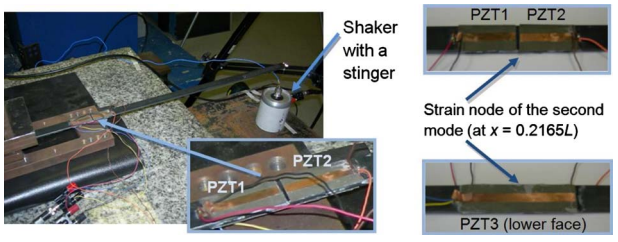

Fig. 5 Experimental setup for demonstration of the effect of strain nodes on the voltage output

Downloaded From: http://vibrationacoustics.asmedigitalcollection.asme.org/ on 09/27/2013 Terms of Use: http://asme.org/terms

excitations at higher modes, which is expected from the theory. For convenience, small PZT patches are used instead of covering the entire surface of the beam. Since the first vibration mode has no strain nodes, we focus on the strain node of the second mode, which is at $x=0.2165L$ as given in Table 1. Therefore, *theoretically*, the distance of this strain node is approximately 130 mm from the clamped end of the beam. Two PZT patches of dimensions 72×19.1 mm^2 are obtained from a monolithic PZT-5A sheet manufactured by Piezo Systems Inc. (as the width of the beam is 19.1 mm and the lengths of the PZT sheets are restricted to 72 mm by the manufacturer). The PZT sheets come from the manufacturer with continuous nickel electrodes. Therefore, in order to realize the idea of *segmented electrodes*, one should either etch the electrodes from the surface of the PZT at the desired location or cut the PZTs to remove the electrical conductivity of the electrodes at the strain node of the beam. The second option is preferred for convenience and one of the two patches is cut into two identical parts to obtain two patches of dimensions 36×19.1 mm^2. First the small patches (PZT1 and PZT2) are attached to the opposite sides of the strain node on the upper surface of the beam (Fig. 5). Then, the longer patch (PZT3) is attached to the lower face of the beam such that the strain node coincides with the center of this patch as shown in Fig. 5. Hence, approximately the same region ($94\leqslant x\leqslant166$ mm) is covered on the upper and the lower surfaces of the beam, and theoretically, the strain node of the second mode is at the center of this region (at $x=130$ mm). Therefore, the PZT and the electrodes are continuous at the lower surface whereas they are discontinuous on the upper surface at the theoretically predicted location of the strain node. In the following discussion, the open circuit voltage across the electrodes is measured in all cases without connecting the electrodes to a harvesting circuit (which corresponds to $R_l\rightarrow\infty$ in the theoretical discussion). For excitations at both vibration modes, the voltage input to the electromagnetic shaker is kept the same.

For excitation at the first natural frequency (which is about 7.1 Hz), the major contribution in Eq. (5) is from the first mode. Therefore, the dynamic strain distribution in PZT3 is expected to be in phase throughout its length since the first mode has no strain nodes. Hence the amplitude of the voltage response across the electrode pair of PZT3 must be identical to the combined amplitude of the voltage responses across the individual electrode pairs of PZT1 and PZT2. The voltage histories across the electrode pairs of PZT1 and PZT2 are shown in Figs. 6(*a*) and 6(*b*), respectively. It is clear from Figs. 6(*a*) and 6(*b*) that the voltage responses of PZT1 and PZT2 are in phase and their amplitudes are also very close to each other.

Figure 6(*c*) shows the voltage response of PZT3 along with the summation of the voltage responses of PZT1 and PZT2 for excitation at the first natural frequency. As expected, the voltage amplitude of PZT3 is approximately identical to the summation of the voltage amplitudes across the electrode pairs of PZT1 and PZT2 as they are in phase. Also, the voltage response of PZT3 is 180 deg out of phase with the summation of PZT1 and PZT2 since the lower face of the beam is in tension when the upper face is in compression, and vice versa. The slight difference in the amplitudes in Fig. 6(*c*) is expected to be due to experimental imperfections. The PZTs were cut by hand and there is a finite spacing between PZT1 and PZT2 as shown in Fig. 5. Figure 6(*c*) is a verification of the fact that PZT patches with continuous electrodes can be used safely for harvesting energy from the first vibration mode since the strain distribution at a thickness level is always in phase over the length of a cantilevered beam.

If the beam is excited at its second natural frequency (which is approximately 40.8 Hz), the dominant vibration mode is the second mode. The voltage outputs of PZT1 and PZT2 are displayed in Figs. 7(*a*) and 7(*b*) for excitation at the second natural frequency. Unlike the voltage outputs for excitation at the first natural frequency, as expected, the voltage outputs of these patches are now 180 deg out of phase with each other. Note that the voltage

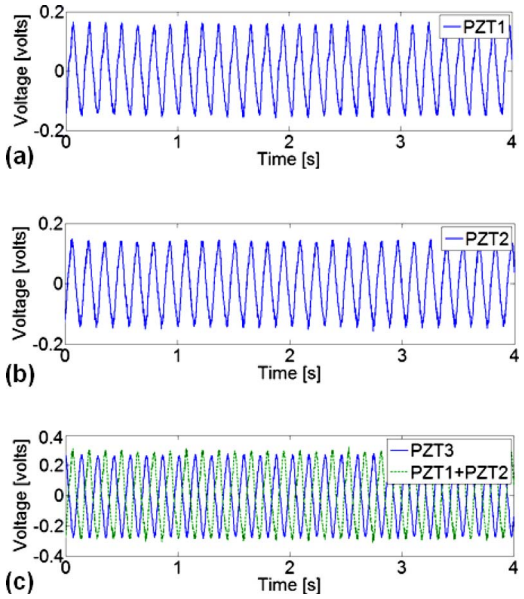

Fig. 6 Voltage histories for excitation at the first natural frequency of the beam: (*a*) PZT1, (*b*) PZT2, and (*c*) PZT3 along with the maximum response obtained by combining PZT1 and PZT2

amplitudes of PZT1 and PZT2 are not identical, which means that the strain distributions at different sides of $x=130$ mm are not identical for excitation at the second natural frequency.

For excitation at the second natural frequency, voltage response across the electrodes of PZT3 is shown in Fig. 7(*c*) along with the appropriate combination of PZT1 and PZT2 outputs for maximum voltage output. Since the charge developed in PZT3 is collected by continuous electrodes, the phase difference in the strain distribution at the opposite sides of the second mode results in cancellation. Therefore the voltage output of PZT3 is less than the individual outputs of PZT1 and PZT2 for the same mechanical input. Clearly, it is not preferable to cover the strain node of a harvester

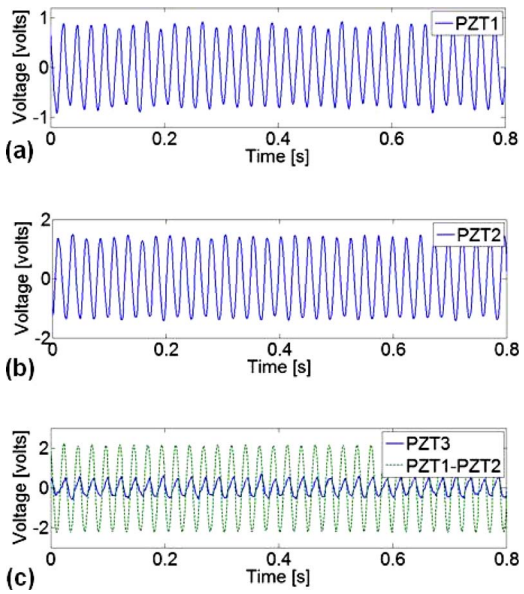

Fig. 7 Voltage histories for excitation at the second natural frequency of the beam: (*a*) PZT1, (*b*) PZT2, and (*c*) PZT3 along with the maximum response obtained by combining PZT1 and PZT2

Downloaded From: http://vibrationacoustics.asmedigitalcollection.asme.org/ on 09/27/2013 Terms of Use: http://asme.org/terms

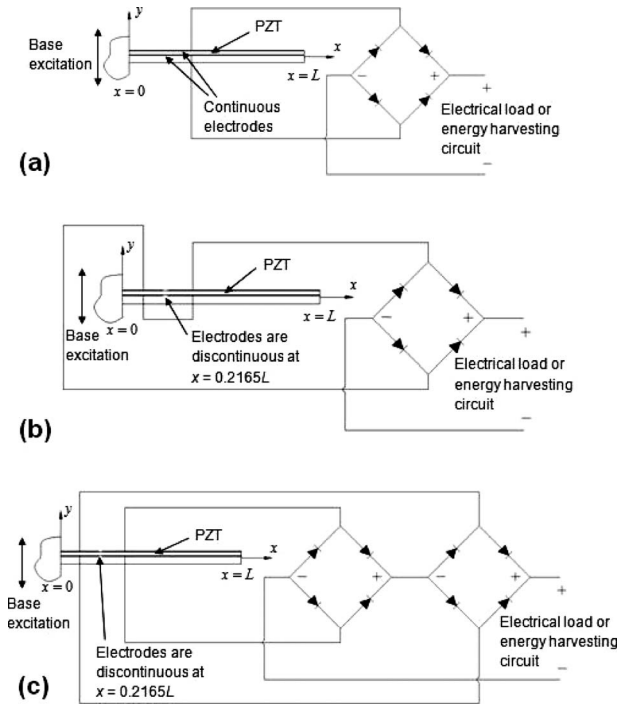

Fig. 8 Continuous and segmented electrode configurations with full-wave rectifiers: (*a*) suitable for mode 1 excitation, (*b*) suitable for mode 2 excitation, and (*c*) suitable for both mode 1 and mode 2 excitations

beam with continuous electrodes. In order to obtain the maximum voltage output from this sample region ($94 \leqslant x \leqslant 166$ mm) for excitation at the second natural frequency, one should collect the electric charge developed in regions $94 \leqslant x \leqslant 130$ mm and $130 \leqslant x \leqslant 166$ mm by separate electrode pairs to obtain the individual voltage outputs of Figs. 7(*a*) and 7(*b*). These voltage outputs can then be combined by considering the phase difference (mathematically, by subtracting the voltage outputs: PZT1-PZT2) to obtain the maximum voltage output (Fig. 7(*c*)). The physical combination of these voltage outputs (i.e., realization of the subtraction PZT1-PZT2) is done by combining the correct leads coming from the respective segmented electrode pairs. The voltage amplitude of the preferable combination of PZT1 and PZT2 is more than four times the amplitude of the voltage response of PZT3.

In this simple example, the continuous electrode pair covering the strain node yielded some voltage output because there is no total cancellation at the opposite sides of $x=130$ mm for PZT3. This fact is in agreement with Fig. 8 since PZT1 and PZT2 outputs do not have the same amplitude. It is worthwhile to add that the position of the strain node ($x=130$ mm) is predicted theoretically and the patches were located on the beam according to this position. Scanning the second mode shape of the beam experimentally and locating the patches according to the strain node of the experimental mode shape would give more accurate results. Also, the PZTs were cut by hand and the region covered by PZT1+PZT2 is not identical to that covered by PZT3 due to the discontinuity between PZT1 and PZT2. Regardless of these experimental imperfections, the qualitative results discussed above are in good agreement with the theory. In conclusion, depending on how they are located on the energy harvester beam and the boundary conditions of the beam, using continuous electrodes may result in dramatically lower electrical outputs in piezoelectric energy harvesting.

4 Relationship With the Energy Harvesting Literature

Recently, Kim et al. [16,17] studied harvesting energy from a *clamped circular plate* due to a pressure drop in an air chamber. Even though their system was not a beam and although they considered the deflection of the plate due to a uniform static pressure rather than its vibrations, Kim et al. [16,17] also observed the cancellation of the electrical outputs when continuous electrodes are used. Based on their theoretical analysis, which uses the energy method, Kim et al. [16] found that no net charge output is obtained if their unimorph circular plate is fully covered by continuous electrodes. They obtained theoretically that, if the electrodes were "regrouped" after $0.707r$ (where r is the radius of the plate), the optimum electrical output could be extracted from the deflection of the PZT due to constant static pressure. Although Kim et al. [16] also mentioned that the problem can be handled by collecting the charge developed in different regions separately and reversing the leads in the electrical circuit, they used the idea of "patterned poling" by changing the direction of polarization of the outer PZT region (that is the region outside a specific radius) in their experimental work [17]. Changing the poling direction implies etching the electrodes at a specific region (at $0.5r$ and $0.75r$ in two separate cases of their work) and then applying a very high electric field in the desired portion of the PZT. After the patterned poling process is completed, Kim et al. [17] used a conductive pen to reconstruct the electrodes at the etched regions. Finally, the electric charge is collected by reconstructed full electrodes and improved results are obtained. They observed experimentally that patterned poling after $0.75r$ gave the best results when compared to the cases of patterned poling after $0.5r$ and the original case with full electrodes and unmodified polarization (in good agreement with their theoretical work [16], which predicted the optimum radius as $0.707r$). It should also be added that the unmodified case with full electrodes still gave some nonzero electric charge output in the order of magnitude of the other cases, most likely because of some physical imperfections, such as realization of the clamped boundaries [17].

It is worthwhile to relate the approach used by Kim et al. [17] to our discussion on cantilevered beams. The optimum location for etching the electrodes is where the electric displacement changes sign and it corresponds to a *strain node* in our study on cantilevered energy harvesters. Once patterned poling process is completed, continuous electrodes can be used for collecting the charge output. Mathematically, as far as our relevant equations for beams are concerned, the piezoelectric constant (e_{31}) changes sign in the modified region after the patterned polarization process. The issue of cancellation in the integral given by Eq. (10) was due to the opposite sign of the curvature at the opposite sides of the strain nodes when e_{31} had the same sign throughout the length of the beam. The new polarization at one side of the strain node makes the sign of the product of the piezoelectric constant and the curvature the same at the opposite sides of the strain node. Hence no cancellation takes place during the integration of the electric displacement over the continuous electrode area. Briefly, in order to avoid the cancellation, either the polarization at one side of the strain node must be reversed (by patterned poling) so that continuous electrodes can be used or the electrodes must be discontinuous at the strain node if the polarization is to be kept the same over the length of the beam (as demonstrated in Sec. 3).

Although the patterned polarization approach solved the *static* deflection problem of Kim et al. [17] *permanently*, it may not be a flexible approach as far as the *dynamic* (vibration) problem is concerned, since the deflection pattern changes with vibration modes. For a simple explanation, consider the second vibration mode of a cantilevered harvester again. If the polarization of the harvester is reversed at one side of the strain node (which is located at $\bar{x}=0.2165$), one can use continuous electrodes (covering $0 \leqslant \bar{x} \leqslant 1$) to collect the charge developed in the PZT and this avoids the cancellation in the integral of Eq. (10) for vibrations

Downloaded From: http://vibrationacoustics.asmedigitalcollection.asme.org/ on 09/27/2013 Terms of Use: http://asme.org/terms

with the second mode shape. After patterned poling, if the beam with continuous electrodes is used for harvesting energy at the first vibration mode, one ends up with a strong cancellation although there is no strain node in the first vibration mode. Even though the curvature has the same sign throughout the beam length for the first mode shape (Fig. 2(*b*)), the change in the sign of e_{31} at $\bar{x}=0.2165$ makes it necessary to consider the integral in Eq. (10) in two parts where cancellation occurs between the two areas ($0 \leq \bar{x} < 0.2165$ and $0.2165 < \bar{x} \leq 1$) under the electric displacement curve. Therefore, in the dynamic problem, the patterned poling process can be favorable for a single vibration mode only. Otherwise, one has to repeat the patterned poling process again in order to use the same harvester beam (which was patterned poled for a certain mode shape) for excitations with another mode shape.

Based on the above discussion, it is reasonable to claim that switching the leads of the segmented electrodes (as described in Sec. 3) is more *flexible* and *reversible* compared to the patterned poling process in the *vibration-based* energy harvesting problem. The patterned poling process can be useful for static problems as a permanent solution since (for a given loading) a single deflection pattern is involved in typical static problems, unlike the vibration problems (where the deflection pattern depends on the vibration mode). Using segmented electrodes is easier to implement as the cancellation problem is mainly solved in the electrical circuit by combining the leads of the electrodes accordingly. Moreover, considering the fact that most PZT patches come with integrated electrodes from the manufacturer, one may not have to apply an etching process to obtain a discontinuity at the strain node of the harvester. In some cases, it may be possible to cut the PZT patch (and therefore its electrodes) as done in our simple experimental demonstration in Sec. 3. The following section discusses handling of the cancellation issue in the electrical circuit for harvesting energy from multiple vibration modes with the same cantilevered energy harvester.

5 Avoiding Cancellation in the Circuit With Segmented Electrodes

The configuration shown in Fig. 8(*a*) is the commonly employed [10,11] ac-dc conversion circuit through a full-wave rectifier where the electrodes bracketing the PZT layer are connected to a diode bridge to remove the sign alternation of the electrical output. In general, a smoothing capacitor is used at the dc side before the electrical load in order to bring the pulsating rectified voltage to a relatively constant value. To be more realistic, instead of a simple resistive load, it is possible to consider a battery/capacitor charging circuit or a more sophisticated adaptive energy harvesting circuit at the dc side, which is beyond the discussion of this paper. Our interest here is to avoid the cancellation of the alternating current output of the PZT before it is supplied to a simple or a sophisticated harvesting circuit. Hence, for convenience, the leads of the dc side are left open in Fig. 8(*a*). As we discussed in the previous sections, if the harvester beam vibrates with the first mode shape, the strain distribution is in phase throughout the length of the beam. Hence, it is possible to collect the charge developed in the PZT with continuous electrodes without cancellation. Considering the strain mode shape of the first mode in Fig. 2(*b*), it can be observed that the main contribution to the electrical output is from the region that is close to the clamped end of the beam. However, covering the entire (top and bottom) faces of the PZT with a continuous electrode pair gives the maximum electrical output and this classical configuration with continuous electrodes (Fig. 8(*a*)) can be used safely as the first vibration mode has no strain nodes.

If the harvester beam vibrates with the second mode shape, using the configuration with continuous electrodes (Fig. 8(*a*)) results in cancellation of the electrical outputs as theoretically discussed and experimentally demonstrated in this paper. In order to avoid the cancellation in a simple manner, segmented electrodes can be used. Figure 8(*b*) shows two segmented electrode pairs used for collecting the electric charge developed in $0 \leq x < 0.2165L$ and $0.2165L < x \leq L$ separately. Note that the bottom electrodes are connected to each other whereas the top electrodes are connected to the diode bridge (series connection). This configuration prevents cancellation in harvesting energy from the second vibration mode because the polarization of the electrodes in these two regions is the opposite of each other all the time during the vibratory motion (i.e., when the top electrode in $0 \leq x < 0.2165L$ is (+), the bottom electrode in $0.2165L < x \leq L$ is also (+), and vice versa). However, if one intends to use the segmented electrode configuration shown in Fig. 8(*b*) for harvesting energy from the first vibration mode, cancellation occurs because of the way the voltage outputs of $0 \leq x < 0.2165L$ and $0.2165L < x \leq L$ are combined. Therefore, the configuration displayed in Fig. 8(*b*) is suitable for vibrations with the second mode shape but it is not preferable for vibrations with the first mode shape.

The configuration given in Fig. 8(*a*) is suitable for harvesting energy from the first mode (but it is not suitable for the second mode) whereas the configuration of Fig. 8(*b*) is suitable for harvesting energy from the second mode (and it is unsuitable for the first mode). However, it is not difficult to combine the outputs of the segmented electrode pairs in Fig. 8(*b*) to come up with a configuration that can be used both for the first mode and second mode vibrations. In the configuration of Fig. 8(*c*), the electrode pairs are connected to two separate diode bridges (again, in the sense of series connection) so that cancellation is prevented regardless of the polarization in the $0 \leq x < 0.2165L$ and $0.2165L < x \leq L$ regions.

The foregoing approach of avoiding the cancellation issue appears to be more flexible and versatile than the patterned polarization technique. Here, the only requirements are the removal of electrodes at the strain nodes and simple considerations in the electrical circuit. The idea described here is not limited to the first two vibration modes and it can easily be extended to higher vibration modes as well (based on the locations of the strain nodes given in Table 1). Alternative circuitry-based approaches can be investigated to handle the cancellation problem for multimode excitations with less number of diodes as the presence of diodes creates losses in the electrical circuit.

6 Effect of Using a Tip Mass on the Electrical Response at Higher Vibration Modes

In many papers on piezoelectric energy harvesting from cantilevered beams, a tip mass is used either to tune the natural frequency of the harvester to a certain value or to improve its structural flexibility by reducing the natural frequencies to practical values especially in microscale applications. Even though exciting a harvester beam harmonically at its first natural frequency is a very useful practice to characterize the device performance and to investigate the electromechanical trends, most ambient vibration sources do not provide a single harmonic input. In general, ambient vibration energy has random frequency behavior and multiple dominant harmonics as in the sample spectra given by Roundy et al. [5]. In some cases, the frequency content of the vibration source varies in time, as measured by Sodano et al. [18] from an automobile compressor. Another type of motion input that is directly available in the ambient is of impulse type (e.g., the lateral acceleration measured at the heel by Erturk et al. [23] during walking). Impulse type of acceleration fluctuation is usually associated with rigid body motions and it excites a broad range of harmonics. Briefly, in practice, it is almost inevitable to avoid higher mode vibrations of a cantilevered harvester even though the optimum case is to excite it at its most flexible mode (which is the first mode). Therefore, this section presents a simple experiment to demonstrate the electrode configuration-based side effect of using a relatively large tip mass on the voltage response of higher vibration modes.

Downloaded From: http://vibrationacoustics.asmedigitalcollection.asme.org/ on 09/27/2013 Terms of Use: http://asme.org/terms

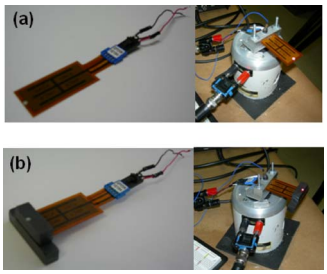

Fig. 9 Piezoelectric bimorph and its experimental base excitation with a shaker in clamped-free boundary conditions: (*a*) without a tip mass and (*b*) with a tip mass

As discussed in Sec. 2.3, a large tip mass makes the free boundary of a cantilevered harvester close to a clamped boundary for vibration modes other than the first mode. Although the attachment of a large tip mass makes the first vibration mode more flexible and improves the voltage response for the fundamental mode excitation, it results in a converse effect by restricting the translation and more importantly the rotation at the free end for excitations at higher mode frequencies. Hence, in the presence of a tip mass with large rotary inertia, a clamped-free harvester starts acting as a clamped-clamped harvester for vibration modes other than the first mode. As discussed extensively in this paper, clamped-clamped boundary conditions with full electrodes can be detrimental to the voltage output of the harvester.

A simple experiment is conducted to demonstrate the trade-off due to using a tip mass for cantilevered harvesters. The experimental setup employs a QuickPack QP25N bimorph manufactured by Mide Technology Corporation. In the absence of a tip mass (Fig. 9(*a*)), the overhang mass of the bimorph is about 2.2 g. A tip mass if 33.5 g is attached to the tip of the bimorph as displayed in Fig. 9(*b*). Such relatively large tip masses and even larger ones have been employed in literature [5], especially for microscale energy harvesting applications [14].

As shown in Fig. 9, an electromagnetic shaker is used to excite the bimorph harvester from its base. The acceleration feedback at the base of the harvester is obtained by a low-mass accelerometer and the tip velocity is measured by a laser vibrometer. A resistive load of 1 kΩ is used to obtain the electrical power frequency response function (FRF) of the bimorph. Figure 10(*a*) shows the tip displacement FRF obtained by using the tip velocity measurement (per base acceleration in *g*) for the configurations with and without the tip mass (Fig. 9). Due to the attachment of the tip mass, the tip displacement is increased only for the first vibration mode and it is attenuated for the higher vibration modes (approximately by a factor of 2 for the second mode and by a factor of 4 for the third mode). Note that the tip motion is strongly attenuated at the off-resonance frequencies of the higher vibration modes as well (the *y*-axis of the plot is in log-scale). Figure 10(*b*) shows the electrical power FRF per square of base acceleration (in *g*). Attachment of the tip mass increases the electrical power output for the first vibration mode. However, it reduces the power output for the second and the third mode excitations by a factor of more than 2 and by a factor of more than 5, respectively. Again, the attenuation in the power output at the off-resonance frequencies is notable, especially by considering the fact that *y*-axis of the plot is given in a log-scale.

The foregoing experimental demonstration shows that attachment of a tip mass suppresses the available vibration-to-electric energy conversion potential for excitations at higher vibration modes, although it improves this potential for the first vibration mode. This trade-off due to using a tip mass can be important if the harvester is excited at the higher vibration modes as well (due to random, varying frequency, or impulse type of excitations). The

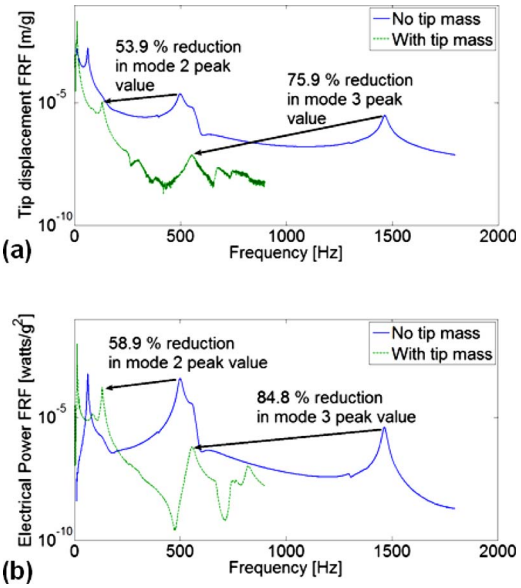

Fig. 10 Experimental comparison of the (*a*) tip displacement and (*b*) electrical power FRFs of the bimorph cantilever configurations with and without the tip mass

cancellation problem at higher modes can be solved by identifying the strain node positions and collecting the electric charge output with segmented electrodes.

7 Summary and Conclusions

Cantilevered beams with piezoceramic layer(s) have been used as piezoelectric energy harvesters for low power generation within the past decade. Typically, a piezoelectric energy harvester is located on a vibrating host structure and the dynamic strain field induced in the piezoceramic layer(s) results in an alternating voltage output across the electrodes. Vibration modes of a cantilevered beam other than the first mode have certain strain nodes where the dynamic strain distribution at a thickness level changes sign in the direction of the beam length. Strain nodes of a vibration mode are simply the inflection points of the eigenfunctions.

In this paper, it is theoretically explained and experimentally demonstrated that covering the strain nodes of vibration modes with continuous electrodes results in cancellation of the electrical outputs. A detailed dimensionless analysis is given for predicting the locations of the strain nodes of a cantilevered beam in the absence of a tip mass. Dimensionless derivations and results are then presented for predicting the strain node positions and their variations in the presence of a tip mass. Since the cancellation problem is not peculiar to clamped-free boundary conditions, dimensionless data of modal strain nodes are tabulated for some other practical boundary condition pairs as well. The locations of strain nodes tabulated in this work are important also for applications of modal actuation since covering these positions with piezoelectric actuator(s) may require very high voltage inputs, yielding inefficient actuation processes.

It is experimentally shown that the voltage output due to the second mode excitation can be increased drastically, if segmented electrodes are used instead of continuous electrodes. The relationship between the discussion given here and a recent study on piezoelectric energy harvesting from the static deflection of a clamped circular plate is also explained. The use of segmented electrode pairs to avoid cancellations is described for single-mode and multimode vibrations of a cantilevered harvester. Alternative circuitry-based approaches can be investigated to handle the cancellation problem for multimode excitations.

In most applications, a tip mass is used either to tune the natural frequency of the harvester to a certain value or to improve its

Downloaded From: http://vibrationacoustics.asmedigitalcollection.asme.org/ on 09/27/2013 Terms of Use: http://asme.org/terms

structural flexibility by reducing the natural frequencies to practical values especially in microscale applications. An electrode configuration-based side effect of using a large tip mass on the voltage response at higher vibration modes is discussed theoretically and demonstrated experimentally. This side effect can be important for random, varying frequency, or impulse type of inputs, where higher modes are excited.

Acknowledgment

The authors gratefully acknowledge the support of the Air Force Office of Scientific Research MURI under Grant No. F 9550-06-1-0326 "Energy Harvesting and Storage Systems for Future Air Force Vehicles" monitored by Dr. B.L. Lee.

References

[1] Williams, C. B., and Yates, R. B., 1996, "Analysis of a Micro-Electric Generator for Microsystems," Sens. Actuators, A, **52**, pp. 8–11.
[2] Beeby, S. P., Tudor, M. J., and White, N. M., 2006, "Energy Harvesting Vibration Sources for Microsystems Applications," Meas. Sci. Technol., **17**, pp. R175–R195.
[3] Anton, S. R., and Sodano, H. A., 2007, "A Review of Power Harvesting Using Piezoelectric Materials (2003–2006)," Smart Mater. Struct., **16**, pp. R1-R21.
[4] Cook-Chennault, K. A., Thambi, N., and Sastry, A. M., 2008, "Powering MEMS Portable Devices—A Review of Non-Regenerative and Regenerative Power Supply Systems with Emphasis on Piezoelectric Energy Harvesting Systems," Smart Mater. Struct., **17**, p. 043001.
[5] Roundy, S., Wright, P. K., and Rabaey, J. M., 2003, "A Study of Low Level Vibrations as a Power Source for Wireless Sonsor Nodes," Comput. Commun., **26**, pp. 1131–1144.
[6] Sodano, H. A., Park, G., and Inman, D. J., 2004, "Estimation of Electric Charge Output for Piezoelectric Energy Harvesting," Integrated Ferroelectrics An International Journal, **40**, pp. 49–58.
[7] duToit, N. E., Wardle, B. L., and Kim, S., 2005, "Design Considerations for MEMS-Scale Piezoelectric Mechanical Vibration Energy Harvesters," Strain An International Journal, **71**, pp. 121–160.
[8] Erturk, A., and Inman, D. J., "On Mechanical Modeling of Cantilevered Piezoelectric Vibration Energy Harvesters," J. Intell. Mater. Syst. Struct., to be published.
[9] Erturk, A., and Inman, D. J., 2008, "A Distributed Parameter Electromechanical Model for Cantilevered Piezoelectric Energy Harvesters," ASME J. Vibr. Acoust., **130**, p. 041002.
[10] Ottman, G. K., Hofmann, H. F., and Lesieutre, G. A., 2003, "Optimized Piezoelectric Energy Harvesting Circuit Using Step-Down Converter in Discontinuous Conduction Mode," IEEE Trans. Power Electron., **18**, pp. 696–703.
[11] Guan, M. J., and Liao, W. H., 2007, "On the Efficiencies of Piezoelectric Energy Harvesting Circuits Towards Storage Device Voltages," Smart Mater. Struct., **16**, pp. 498–505.
[12] 1987, *IEEE Standard on Piezoelectricity*, IEEE, New York.
[13] Beer, F. P., and Johnston, E. R., Jr. 1992, *Mechanics of Materials*, McGraw-Hill, New York.
[14] Fang, H.-B., Liu, J.-Q., Xu, Z.-Y., Dong, L., Chen, D., Cai, B.-C., and Liu, Y., 2006, "A MEMS-Based Piezoelectric Power Generator for Low Frequency Vibration Energy Harvesting," Chin. Phys. Lett., **23**, pp. 732–734.
[15] Elvin, N. G., Elvin, A. A., and Spector, M., 2001, "A Self-Powered Mechanical Strain Energy Sensor," Smart Mater. Struct., **10**, pp. 293–299.
[16] Kim, S., Clark, W. W., and Wang, Q. M., 2005, "Piezoelectric Energy Harvesting with a Clamped Circular Plate: Analysis," J. Intell. Mater. Syst. Struct., **16**, pp. 847–854.
[17] Kim, S., Clark, W. W., and Wang, Q. M., 2005, "Piezoelectric Energy Harvesting With a Clamped Circular Plate: Experimental Study," J. Intell. Mater. Syst. Struct., **16**, pp. 855–863.
[18] Sodano, H. A., Inman, D. J., and Park, G., 2005, "Generation and Storage of Electricity from Power Harvesting Devices," J. Intell. Mater. Syst. Struct., **16**, pp. 67–75.
[19] Erturk, A., and Inman, D. J., 2008, "An Experimentally Validated Bimorph Cantilever Model for Piezoelectric Energy Harvesting From Base Excitations," Smart Mater. Struct., in review.
[20] Cady, W. G., 1946, *Piezoelectricity: An Introduction to the Theory and Applications of Electromechanical Phenomena in Crystals*, McGraw-Hill, New York.
[21] Crawley, E. F., and de Luis, J., 1987, "Use of Piezoelectric Actuators as Elements of Intelligent Structures," AIAA J., **25**, pp. 1373–1385.
[22] Lesieutre, G. A., and Davis, C. L., 1997, "Can a Coupling Coefficient of a Piezoelectric Device Be Higher Than Its Active Material," J. Intell. Mater. Syst. Struct., **8**, pp. 859–867.
[23] Erturk, A., Anton, S. R., and Inman, D. J., 2007, "Energy Harvesting from Rigid Body Motions," *Proceedings of the 18th International Conference of Adaptive Structures and Technologies*, Ottawa, ON, Canada, on CD.

Downloaded From: http://vibrationacoustics.asmedigitalcollection.asme.org/ on 09/27/2013 Terms of Use: http://asme.org/terms